DETERIORATION ASSESSMENT OF LOW-DENSITY POLYETHYLENE-STARCH-IONOMER MIXTURES CONTAINING METAL STEARATES

Zeena P. Hamza[1*], Thomas Kurian[2]

Abstract

Ferric stearate, manganese stearate, cupric stearate, magnesium stearate and zinc stearate were introduced to zinc salt of poly (ethylene-co-methacrylic acid) (5%) compatible low density polyethylene-starch blends in different weight percentages (0.5 and 1 weight%). The role of trace amounts of metal stearates as pro-oxidants in the blends was evaluated using mechanical properties, melt flow indices, biodegradability, photodegradability, photobiodegradability, water absorption, infrared spectroscopy, dynamic mechanical analysis, thermogravimetry, differential scanning calorimetry, and scanning electron microscopy. The mechanical properties of the mixes were altered by the addition of metal stearates. The addition of metal stearates altered the thermal stability and crystallinity, according to thermal characterization performed with TGA and DSC. A number of degradative studies indicate that adding metal stearates enhances the blends' capacity to degrade, that were confirmed by SEM micrographs.

Keywords: ionomer, pro-oxidant, biodegradability, photodegradability, photo biodegradability

[1*]Department of Chemistry, Govt. College, Kattappana, Idukki, Kerala, India, 685508
[2]Department of Polymer Science and Rubber Technology, Cochin University of Science and Technology, Kochi, Kerala, India, 682022

Corresponding author: Dr. Zeena P. Hamza
*Emails: zeenaphamza@gmail.com

Eur. Chem. Bull. 2022, 11(Regular Issue 1), 608-621

608

INTRODUCTION

These days, there is a growing interest in the oxidative-biodegradation of polymers utilized in packaging applications. One common polyolefin polymer used in packaging is low density polyethylene. Low density polyethylene's hydrophobicity, high molecular weight, and absence of functional groups recognised by microbial enzymatic systems are factors contributing to its resistance to biodegradation. Due to these characteristics, these materials cannot be used in applications where biodegradability is a desired characteristics [1-2]. One feasible solution to hasten the microbes' assault on LDPE is to allow natural polymers, like starch, to accumulate and ensure at least partial biodegradation. Starch is a good option since it's a cheap and readily available raw material [3]. The two main methods developed to overcome low density polyethylene's inherent resistance to biological attack are the insertion of functional groups into the polyethylene backbone and the blending of polyethylene with photo-initiating pro-oxidants capable of promoting the formation of free radical precursor moieties by photo-oxidation to induce cleavage of the macromolecular backbone [4].

Low density polyethylene-starch blends containing pro-oxidants undergo photo-oxidation, which raises the low molecular weight fraction through chain scission and accelerates biodegradation [5-7]. Additionally, because to embrittlement and the ensuing track growth, it increases the surface area. Moreover, polyethylene becomes more hydrophilic when carbonyl groups form on its surface [8]. Transition metals have been reported to be effective photoinitiators for polyethylene [9]. Most commercial photodegradable compositions contain transition metals, especially iron and manganese, because of their exceptional capacity to degrade the hydroperoxides produced during the oxidation process of polymers [10–11].

Curiously, adding starch to LDPE can increase its biodegradability, but it can also change the blend's mechanical characteristics. For example, adding more starch to LDPE may result in a decrease in impact strength and Young's modulus, two properties essential to agricultural plastics' longevity [12]. Compatibilizers, however, can improve the LDPE and starch interfacial properties enhancing the blends' tensile strength and elongation at break [13-15].

The present study examines the effect of metal stearates (ferric stearate, manganese stearate, cupric stearate, magnesium stearate and zinc stearate), to enhance the degradative properties of low density polyethylene-starch blends that are compatible with zinc salt of poly (ethylene-co-methacrylic acid) ionomer, EMA-Zn. The sample designations and descriptions used in this work are displayed in Table 1. The films were characterized by mechanical properties, scanning electron microscopy, thermal properties, and infrared spectroscopy. We also examined the films' photodegradability, biodegradability, and photobiodegradability.

Table 1. Description of sample designations

Sample designation	Description
LDS-Zn	LDPE-20% starch-5% (EMA-Zn)
LDS-Zn-Fe	LDPE-20% starch-5% (EMA-Zn)- ferric stearate
LDS-Zn-Mn	LDPE-20% starch-5% (EMA-Zn)- manganese stearate
LDS-Zn-Cu	LDPE-20% starch-5% (EMA-Zn)- cupric stearate
LDS-Zn-Mg	LDPE-20% starch-5% (EMA-Zn)- magnesium stearate
LDS-Zn-Zn	LDPE-20% starch-5% (EMA-Zn)- zinc stearate

MATERIALS AND METHODS
Materials
Low density polyethylene (LDPE)

The film grade low density polyethylene (LDPE 24FS040) was supplied by Periyar Polyfilms, Edayar, Kerala, India, and came from Reliance Industries Limited, Mumbai, India. It had a melt flow index (190 °C/2.16 kg) of 4 g/10 min and a density (23 °C) of 0.922 g/cm3.

Starch

The supplier of the tapioca starch (300 and 100 mesh) was Jemsons Starch & Derivatives located in Aroor, Alappuzha, Kerala. These fillers were oven dried at 120 °C for one hour before combining because they were hygroscopic in nature.

Ionomers

Zinc salt of poly(ethylene-co-methacrylic acid) (HIMILAN 1702 EMAAZn), with a melt flow index (190 °C/2.16 kg) of 16 g/10 min, was the ionomer employed in this investigation. The Japanese company Mitsubishi Plastics, Inc. provided these ionomers.

Pro-oxidants

Eur. Chem. Bull. 2022, 11(Regular Issue 1), 608-621

609

Specifically, pro-oxidants such as ferric, manganese, cupric, magnesium, and zinc stearates were employed in this investigation. The supplier of ferric, manganese, and copper stearate was Jingjiang Concord Plastics Technology Co. Ltd. in China. Alfa Chemicals, located in Ernakulam, Kerala, India, provided the zinc and magnesium stearate.

Methods
Preparation of blends
Melt mixing was performed using a Thermo Haake Polylab system (Rheocord 600p) with roller-type rotors. The volumetric capacity of the mixing chamber is 69 cm^3. All of the compounds were mixed for eight minutes at 150 °C and 30 rpm of rotor speed. The filler was added after the LDPE and ionomer had melted for two minutes. Six more minutes were spent mixing.

Preparation of test specimens
To construct the test specimens, the compounds and neat LDPE were molded for five minutes at 150 °C and 20 MPa of pressure in an electrically heated hydraulic press. After being moulded, samples were cooled under pressure to room temperature.

Characterization
Mechanical properties
With a crosshead speed of 50 mm/min, the mechanical properties were assessed with a Shimadzu Autograph AG-I series universal testing equipment. Measurements were made in accordance with ASTM D-882 (2002) for tensile strength, elongation at break, and elastic modulus. Every data point was represented by the average of at least five sample readings.

Melt Flow Index (MFI)
A CEAST Modular Line Melt Flow Indexer was used to measure the melt flow index (MFI) of each blend of LDPE with filler in compliance with ASTM method D-1238. A 2.16 kg load was applied at a melt temperature of 190 °C.

Biodegradation studies
The mixes' biodegradation investigations were conducted in compliance with ASTM D-6691. The Microbial Genetic Lab, Department of Biotechnology, Cochin University of Science and Technology provided the bacterial cultures. Sediment samples taken from several spots in the Mangalavanam mangroves and Cochin backwaters were used to isolate these microorganisms. According to Bergey's Manual of Systematic Bacteriology [16], the morphological and biochemical properties of these cultures led to their earlier classification as members of the genus Vibrionacea. They were preserved using the paraffin oil overlay method in glass 10 mL bottles. The consortium isolates were cultivated individually at 37 °C and 120 rpm for the entire night on an Orbitek shaker (Scigenics Pvt. Ltd, Chennai, India) in nutritional broth (Himedia, Mumbai) with a pH of 7.0 ± 0.3 and 1% NaCl to prepare the inoculum. Centrifugation was used to extract the cells, which were then pooled after being spun at 5000 rpm (2292 g) for 20 minutes. A 50 mL amylase minimum medium devoid of starch was inoculated with 5 mL of this pooled culture (OD660 = 1). Samples made from blends that had been cleaned with 70% alcohol were introduced to this medium, and these strips served as the only carbon source. For three months in total, the incubation was conducted in the Orbitek environmental shaker at 37 °C and 120 rpm. The medium without the inoculum with corresponding starch-plastic blends and subjected to the same treatment as above were used as controls.

The soil burial test was also carried out to evaluate the biodegradability of the blends. Water absorption was measured using 3 x 1 inch film strips of <1mm thickness according to ASTM D-570-81 method.

Photodegradation by UV rays
In this study, plastic film samples were cut into 8x1 cm pieces and exposed to a 30-watt shortwave UV lamp at a distance of 30 cm for one month. Tensile strength was then determined using a universal testing machine. The average weight of the test specimens was measured using a Sartorius-0.1 mg electronic balance before and after the degradation studies.

Fourier transform infrared spectroscopy (FTIR)
The FTIR spectra of the samples were recorded in the transmittance mode using a Thermo Nicolet, Avatar 370 FTIR spectrophotometer in the spectral range of 4000–400 cm^{-1}.

Dynamic mechanical analysis (DMA)
Utilizing TA Instruments' Dynamic Mechanical Analyzer (DMA Q-800), the samples' viscoelastic characteristics were examined. One Hz was the constant frequency used for DMA analysis. A temperature ramp was conducted between 40 °C and 100 °C in order to obtain a general understanding of the materials' thermomechanical

Eur. Chem. Bull. 2022, 11(Regular Issue 1), 608-621

610

behavior. Measurements were made of the tan δ, loss modulus, and dynamic storage modulus.

Thermogravimetric analysis (TGA)

A nitrogen environment was used for the thermogravimetric analysis, which was performed in a TGA Q-50 thermal analyzer (TA Instruments). The samples were heated at a rate of 20 °C per minute from room temperature to 600 °C while receiving a flow rate of 40–50 cm³/min of nitrogen gas. Sample weights ranged from 10 to 15 milligrams. The ultrasensitive microbalance was used to record the weight changes. Using the Q Series Explorer software from TA Instrument, weight loss data were recorded online in relation to temperature and time. Using the Universal Analysis 2000 software version 3.3 B from TA Instrument, the thermogravimetric (TG) curves were analyzed. T_{max}, or the temperature at which weight loss is greatest, was measured.

Differential scanning calorimetry (DSC)

Using a TA Q-100 thermal analyzer (TA Instruments) in a nitrogen environment and a heating rate of 10 °C/min, the crystallinity of the samples was investigated. To remove the thermal history, samples weighing 5–10 mg were heated in a nitrogen environment from -50 °C to 150 °C for three minutes. The next step involved cooling from 150 °C to -50 °C, and then heating again at the same pace from -50 °C to 150 °C. Using the DSC traces, the percentage of crystallinity was computed as follows.

$$\% \text{ Crystallinity} = (\Delta H_{f\,(obs)} / \Delta H_{f\,(100\%\,crystalline)}) \times 100$$

where $\Delta H_{f\,(obs)}$ is the enthalpy associated with melting of the material and $\Delta H_{f\,(100\%\,crystalline)}$ is the enthalpy of 100% crystalline polyethylene reported in the literature to be 286.7J/g.

Morphological studies

Within 24 hours of the fractures, the tensile fractured surfaces in this study were sputter-coated with platinum in a JFC 1600 Autofine coater, and subsequently analyzed using a JEOL model JSM-6390LV scanning electron microscope (SEM). The surfaces were mounted on a metallic stub with the assistance of silver tape and conducting paint in an upright position.

RESULTS AND DISCUSSION
Mechanical properties

Figure 1. displays the tensile strength, elongation at break, and elastic modulus of the purified LDPE, the LDPE-starch-(EMA-Zn) mix, and the blends that incorporate metal stearates as pro-oxidants. When LDPE-starch-(EMA-Zn) blends with metal stearates are included, the blend with ferric stearate exhibits a little increase in tensile strength when compared to the LDPE-starch-(EMA-Zn) mix. When comparing the tensile strength of the compositions including the other metal stearates (figure 1(a)) to LDPE-starch-(EMA-Zn), they were almost identical.
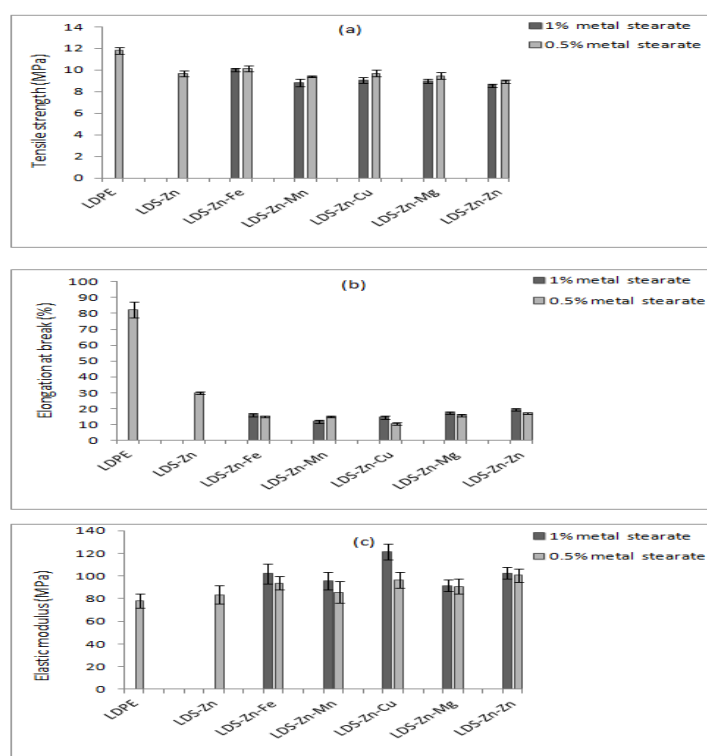

Figure 1. Effect of metal stearates on the mechanical properties of LDPE-starch-(EMA-Zn) blends

Eur. Chem. Bull. 2022, 11(Regular Issue 1), 608-621

611

In comparison to the basic material (LDPE-starch-ionomer blends), Figure 1(b). demonstrates that the addition of metal stearates resulted in a decrease in the elongation at break. The blends including metal stearates exhibited an increase in elastic modulus, as shown in Figure 1(c). Notably, all blends had values higher than the LDPE-starch-ionomer mix. This reflects the degree of compatibility and the existence of stiff materials [17].

Processability of a polymer is commonly assessed using its melt flow index (MFI), which is correlated with its molecular weight distribution. The impact of metal stearates on the melt flow indices of blends of LDPE, starch, and (EMA-Zn) is depicted in Figure 2. All of the samples' MFI values rose when compared to the MFI value of plain LDPE, a sign of chain scission at high temperatures in the presence of metal stearates. The findings indicate that metal stearate-containing LDPE-starch-(EMA-Zn) blends are more prone to deterioration.
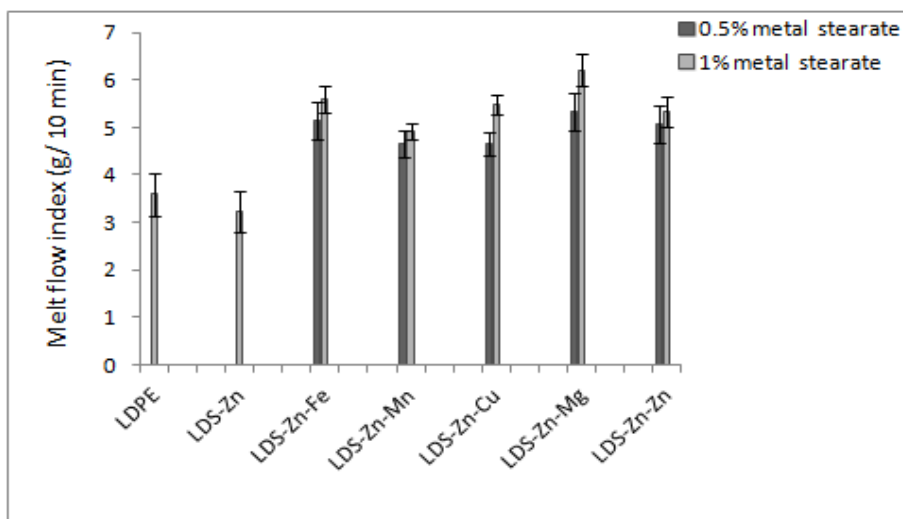
Melt flow measurements

Figure 2. Effect of metal stearates on the melt flow indices of LDPE-starch-(EMA-Zn) blends

Biodegradation studies
The tensile characteristics of LDPE-starch-(EMA-Zn)-metal stearate blends following two months of biodegradation in culture media are displayed in Figures 3. The % decline in tensile strength for

LDPE-starch-EMA-Zn-metal stearate blends is displayed in Tables 2. Following biodegradation, the tensile strength of each mix significantly decreases.
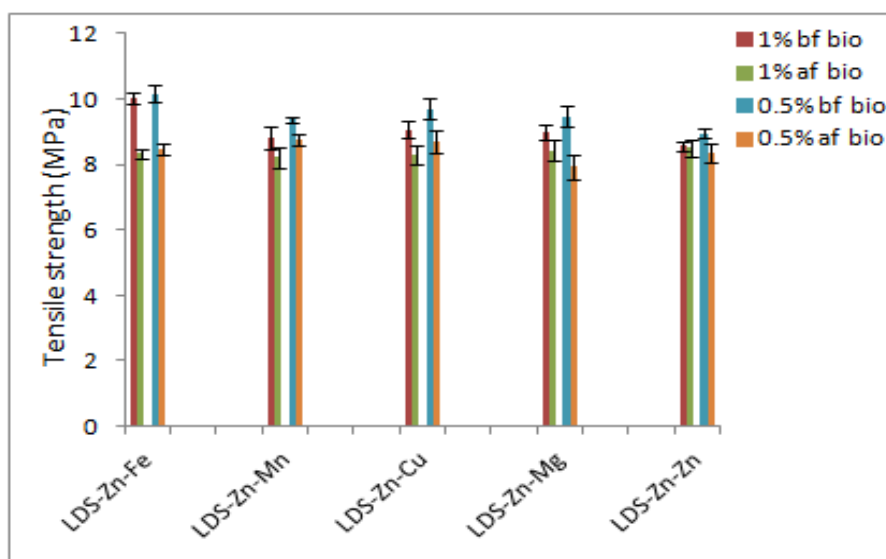

Figure 3. Biodegradation of LDPE-starch-(EMA-Zn)-metal stearate blends after biodegradation in culture medium for two months (Evident from tensile strength)

Table 2.   Percentage decrease in tensile strength of LDPE-starch-(EMA-Zn)-metal stearate blends after biodegradation in culture medium for two months

Sample	Initial tensile strength (MPa)	Tensile strength after biodegradation for two months (MPa)	% decrease in tensile strength
LDS-Zn(1)Fe*	10.1 ± 0.17	8.33 ± 0.15	17.53
LDS-Zn((0.5))Fe	10.2 ± 0.26	8.46 ± 0.18	17.06
LDS-Zn(1)Mn	8.90 ± 0.35	7.62 ± 0.31	14.38
LDS-Zn(0.5)Mn	9.38 ± 0.08	8.26 ± 0.16	11.94
LDS-Zn(1)Cu	9.06 ± 0.26	7.68 ± 0.30	15.28
LDS-Zn(0.5)Cu	9.71 ± 0.31	8.51 ± 0.33	12.36
LDS-Zn(1)Mg	8.98 ± 0.23	8.12 ± 0.32	9.58
LDS-Zn(0.5)Mg	9.48 ± 0.31	8.73 ± 0.35	7.91
LDS-Zn(1)Zn	8.56 ± 0.15	7.96 ± 0.22	7.01
LDS-Zn(0.5)Zn	8.96 ± 0.16	8.370 ± 0.28	6.59

* Number given in paranthesis denotes the weight percentage of metal oxides in the blend

The decrease can be attributed to microbes' consumption of starch. The tensile characteristics of the mix films exhibit these changes, indicating a potential for partial biodegradation of the blends.
.

Tables 3. provide an overview of the blends' % weight loss during biodegradation in culture medium. The LDPE-starch-ionomer blends containing metal stearates are partially biodegradable, as shown by the considerable weight loss that all of the samples showed following breakdown in culture media

Table 3. Percentage decrease in weight of LDPE-starch-(EMA-Zn)-metal stearate blends after biodegradation in culture medium for two months

Sample	Initial weight (g)	Weight after two months (g)	% weight loss
LDS-Zn(1)Fe	0.3905	0.3749	4.01
LDS-Zn((0.5))Fe	0.4808	0.4683	2.60
LDS-Zn(1)Mn	0.5420	0.5265	2.87
LDS-Zn(0.5)Mn	0.6531	0.6359	2.64
LDS-Zn(1)Cu	0.6057	0.5948	1.79
LDS-Zn(0.5)Cu	0.4397	0.4314	1.88
LDS-Zn(1)Mg	0.4950	0.4813	2.76
LDS-Zn(0.5)Mg	0.4834	0.4684	3.10
LDS-Zn(1)Zn	0.7460	0.7274	2.49
LDS-Zn(0.5)Zn	0.5202	0.5050	2.92

Photodegradation studies

Eur. Chem. Bull. 2022, 11(Regular Issue 1), 608-621
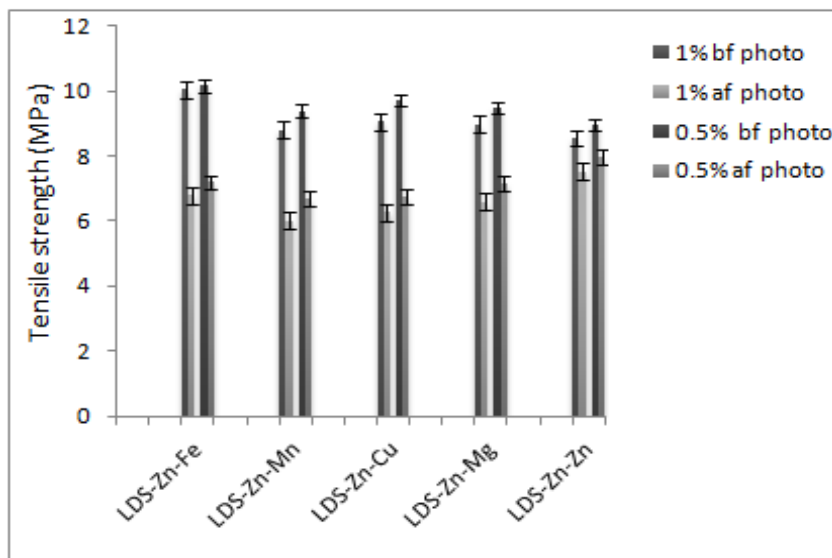
613

Figure 4. Photodegradation of LDPE-starch-(EMA-Zn)-metal stearate blends after UV exposure for one month (Evident from tensile strength)

Table 4. Percentage decrease in tensile strength of LDPE-starch-(EMA-Zn)-metal stearate blends after UV exposure for one month

Sample	Initial tensile strength (MPa)	Tensile strength after UV exposure for one month (MPa)	% decrease in tensile strength
LDS-Zn(1)Fe	10.1 ± 0.17	6.78 ± 0.25	32.47
LDS-Zn((0.5))Fe	10.2 ± 0.26	7.19 ± 0.30	29.50
LDS-Zn(1)Mn	8.81 ± 0.35	6.02 ± 0.23	31.67
LDS-Zn(0.5)Mn	9.38 ± 0.08	6.68 ± 0.28	28.79
LDS-Zn(1)Cu	9.06 ± 0.26	6.26 ± 0.19	30.91
LDS-Zn(0.5)Cu	9.71 ± 0.31	6.76 ± 0.28	30.38
LDS-Zn(1)Mg	8.98 ± 0.23	6.59 ± 0.12	26.62
LDS-Zn(0.5)Mg	9.48 ± 0.31	7.17 ± 0.15	24.37
LDS-Zn(1)Zn	8.56 ± 0.15	7.52 ± 0.24	12.15
LDS-Zn(0.5)Zn	8.96 ± 0.16	7.96 ± 0.23	11.15

The tensile characteristics of LDPE-starch-(EMA-Zn)-metal stearate blends following a month of UV exposure are displayed in Figure 4. The % decline in tensile strength for LDPE-starch-(EMA-Zn)-metal stearate blends is displayed in Table 4.

Table 5. Percentage decrease in weight of LDPE-starch-(EMA-Zn)-metal stearate blends after UV exposure for one month

Sample	Initial weight (g)	Weight after one month (g)	% weight loss
LDS-Zn(1)Fe	0.5867	0.5826	0.699
LDS-Zn((0.5))Fe	0.8243	0.8217	0.315
LDS-Zn(1)Mn	0.5060	0.5013	0.929
LDS-Zn(0.5)Mn	0.5933	0.5910	0.388
LDS-Zn(1)Cu	0.5601	0.5592	0.161
LDS-Zn(0.5)Cu	0.5706	0.5700	0.105
LDS-Zn(1)Mg	0.4819	0.4804	0.311
LDS-Zn(0.5)Mg	0.5873	0.5872	0.017
LDS-Zn(1)Zn	0.6251	0.6231	0.320
LDS-Zn(0.5)Zn	0.7764	0.7744	0.258

Tensile strength significantly decreases after one month of UV radiation exposure. One possible explanation for the decrease in tensile strength could be the formation of new groups in the

polymer chain, primarily in the amorphous region of the material, as a result of the blend's altered chemical structure following exposure to ultraviolet radiation [18]. After a month of UV exposure, the percentage weight loss for blends of LDPE, starch, ionomer, and metal stearate is displayed in Table 5. All of the samples were found to have a slight weight decrease following photodegradation and

Photodegradation studies
Following photobiodegradation investigations, the tensile characteristics of LDPE-starch-(EMA-Zn)-metal stearate blends are displayed in Figure 5. The

process of photobiodegradation was examined by subjecting the samples to UV light for a month and then immersing them in culture media containing amylase-producing *Vibrios,* which were isolated from the marine benthic environment, for an additional month. The percentage decline in tensile strength for LDPE-starch-(EMA-Zn)-metal stearate blends is displayed in Table 6. After two months of photobiodegradation, the tensile strength significantly decreases. This is due to the polyethylene-starch blend's photo-oxidation, which contains pro-oxidants and increases the low molecular weight fraction by chain scission, promoting biodegradation [9].
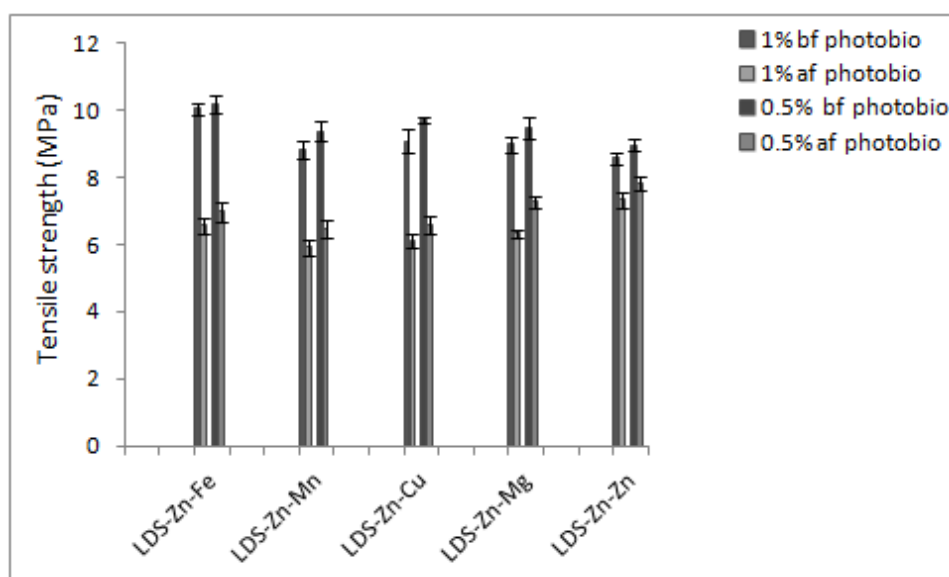

Figure 5. Variation in tensile strength of LDPE-starch-(EMA-Zn)-metal stearate blends after UV exposure for one month followed by biodegradation in culture medium for one month

Table 6. Percentage decrease in tensile strength of LDPE-starch-(EMA-Zn)-metal stearate blends after UV exposure for one month followed by biodegradation in culture medium for one month

Sample	Initial tensile strength (MPa)	Tensile strength after photobiodegradation for two months (MPa)	% decrease in tensile strength
LDS-Zn(1)Fe	10.1 ± 0.17	6.56 ± 0.25	35.04
LDS-Zn((0.5))Fe	10.2 ± 0.26	6.98 ± 0.30	31.53
LDS-Zn(1)Mn	8.90 ± 0.35	5.91 ± 0.23	32.88
LDSs-Zn(0.5)Mn	9.38 ± 0.08	6.45 ± 0.28	31.20
LDS-Zn(1)Cu	9.06 ± 0.26	6.10 ± 0.19	32.65
LDS-Zn(0.5)Cu	9.71 ± 0.31	6.59 ± 0.28	32.10
LDS-Zn(1)Mg	8.98 ± 0.23	6.34 ± 0.12	29.40
LDS-Zn(0.5)Mg	9.48 ± 0.31	7.26 ± 0.15	23.41
LDS-Zn(1)Zn	8.56 ± 0.15	7.33 ± 0.24	14.43
LDS-Zn(0.5)Zn	8.96 ± 0.16	7.82 ± 0.23	12.78

Table 7. summarizes percentage weight loss of the blends during biodegradation in culture medium. Following photobiodegradation, all of the samples

showed a notable decrease in weight. This can be attributed to the oxidation products' microbial breakdown.

Table 7. Percentage decrease in weight of LDPE-starch-(EMA-Zn)-metal stearate blends after UV exposure for one month followed by biodegradation in culture medium for one month

Eur. Chem. Bull. 2022, 11(Regular Issue 1), 608-621

615

Sample	Initial weight (g)	Weight after two months (g)	% weight loss
LDS-Zn(1)Fe	0.5867	0.5758	1.86
LDS-Zn((0.5))Fe	0.8243	0.8123	1.46
LDS-Zn(1)Mn	0.5060	0.4969	1.80
LDS-Zn(0.5)Mn	0.5933	0.5879	0.91
LDS-Zn(1)Cu	0.5601	0.5526	1.34
LDS-Zn(0.5)Cu	0.5706	0.5631	1.31
LDS-Zn(1)Mg	0.4819	0.4736	1.72
LDS-Zn(0.5)Mg	0.5873	0.5814	1.01
LDS-Zn(1)Zn	0.6251	0.6133	1.89
LDS-Zn(0.5)Zn	0.7764	0.7630	1.73

Water absorption studies

Table 8. shows the properties of water absorption for mixes of LDPE, starch, ionomer, and metal stearate. With a rise in metal stearate concentration, the tendency to absorb water reduces. One possible explanation for this could be that the metal stearate particles are occupying the free volume within the polymer matrix, obstructing the entry of water molecules.

Table 8. Water absorption of LDPE-starch-(EMA-Zn)-metal stearate blends

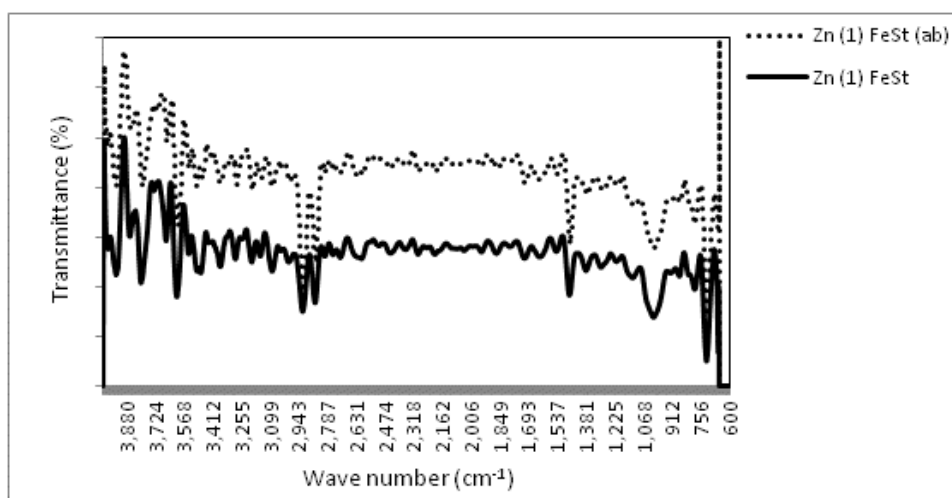| Sample	Initial weight (g)	Weight after 24 hours (g)	% water absorption
LDS-Zn(1)Fe	0.2848	0.2888	1.41
LDS-Zn((0.5))Fe	0.3601	0.3652	1.42
LDS-Zn(1)Mn	0.3223	0.3262	1.21
LDS-Zn(0.5)Mn	0.2711	0.2747	1.33
LDS-Zn(1)Cu	0.3759	0.3798	1.04
LDS-Zn(0.5)Cu	0.4548	0.4604	1.23
LDS-Zn(1)Mg	0.3270	0.3304	1.04
LDS-Zn(0.5)Mg	0.3027	0.3062	1.16
LDS-Zn(1)Zn	0.5174	0.5218	0.85
LDS-Zn(0.5)Zn	0.3804	0.3837	0.87

FTIR spectroscopy

Figure 6. FTIR spectra of LDPE-starch-(EMA-Zn)- 1% ferric stearate blend:
(─) before biodegradation and (…) after biodegradation (ab)

Table 9. Characteristic FTIR spectral peaks

	Peak position (cm^{-1})	Characteristic group
LDPE-starch-(EMA-Zn)-1% ferric stearate	2915, 2847	C-H symmetric stretching
	1535	C=O stretching
	1463	CH$_2$ scissor and asymmetric bending
	1373	C-H bending
	1006	O-C stretching
	912	O-H deformation
	717	CH$_2$ rocking

The FTIR spectra of LDPE-starch-(EMA-Zn) blend with 1% ferric stearate are shown in Figure 6. The spectra display distinctive absorption peaks, listed in Table 9. The stretching vibrations of O-H in the water molecules are responsible for the peaks in the 3700-3200 cm^{-1} area. C-H stretching is the cause of the doublet peaks seen in the 2965-2800 cm^{-1} range [19]. Stearates typically have carboxylate asymmetric stretching vibration bands in the vicinity of 1540 cm^{-1}. Peak intensities at 2921–2848 cm^{-1}, 1473–1463, 1156–1028 cm^{-1}, and 730–720 cm^{-1} showed some improvement following two months of biodegradation in culture medium. This was presumably because the polyethylene chain broke in degradable settings, increasing the number of terminal groups.

The symmetrical stretching vibration of C-H bonds, the bending vibration of moderate intensity C-H bonds, and the distinctive absorption of the crystalline and amorphous bands are responsible for the peaks at 2921-2848 cm^{-1}, 1473-1463 cm^{-1}, and 730-720 cm^{-1}.

The C-O-C bond stretching of starch is responsible for the peaks at 1028 and 1156 cm^{-1}, while the distinctive peak of the O-C stretch is located close to 1019 cm^{-1}. The biodegradation of blends containing ferric stearate is indicated by the presence of significant differences following biodegradation in these areas.

Dynamic mechanical analysis
The changes in the storage modulus and loss factor (tan δ) of LDPE-starch-(EMA-Zn) blends with metal stearates, measured between 40^{0}C and 100^{0}C, are displayed in Figure 7. The strorage modulus values increased with the addition of metal stearates, suggesting that the blends' interfacial contact between phases was improved [20].
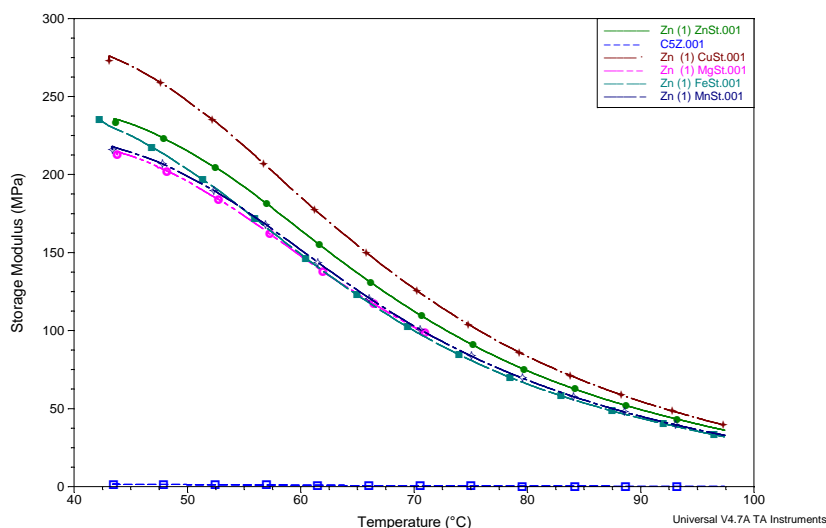

Figure 7. DMA curves of LDPE-starch-(EMA- Zn)-1% metal stearate blends

Thermogravimetric analysis

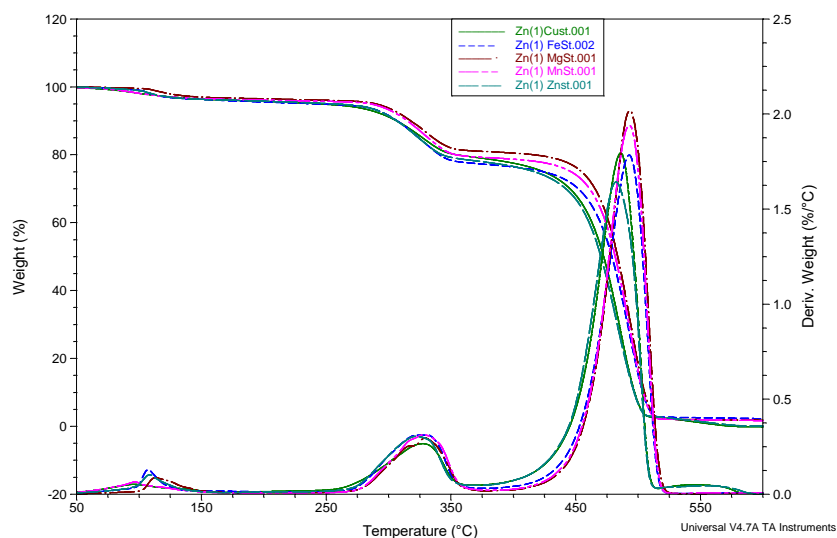*Eur. Chem. Bull. 2022, 11(Regular Issue 1), 608-621*

617

Figure 8. TGA thermograms of LDPE-starch-(EMA-Zn)-1% metal stearate blends

Table 10. TGA results for LDPE-starch-(EMA-Zn)-1% metal stearate blends

Sample	Temperature of onset of degradation (^{0}C)	T_{max} (^{0}C)	Rate of maximum degradation (%/^{0}C)	Residual weight (%)
LDS-Zn	431.28	490.07	2.082	1.209
LDS-Zn(1)Fe	428.86	492.64	1.784	2.273
LDS-Zn(1)Mn	424.78	492.66	1.941	1.681
LDS-Zn(1)Cu	407.10	485.88	1.795	0.1312
LDS-Zn(1)Mg	434.58	493.18	2.018	1.792
LDS-Zn(1)Zn	413.26	482.06	1.643	0.0784

The blends of LDPE-starch-(EMA-Zn)-1% metal stearate show many breakdown zones in their thermograms, which are shown in Figure 8. The thermal breakdown of the low molecular weight components in the blends can be attributed to the first weight loss area, which is located at about 100^{0}C. The majority of the starch was thermally degraded in the second weight loss region, which ranged from 250^{0}C to 350 ^{0}C. The primary decomposition zone, responsible for the third weight loss, is situated between 420^{0}C and 525^{0}C and is linked to the thermal breakdown of pure polyethylenes' backbone chains. Table10. displays the degradation rate, weight of residue, maximum decomposition temperature (T_{max}), and temperature at which degradation first occurs. The findings indicate that adding metal stearates lowers the temperature at which all LDPE-starch-(EMA-Zn) blends begin to degrade, with the exception of the blend that contains magnesium stearate as a pro-oxidant. However, the thermogravimetric characteristics of pure LDPE (T_{onset} = 420^{0}C, T_{max} = 482^{0}C) are altered throughout the blending

process. Moreover, for any blend of LDPE, starch, ionomer, and metal stearate, the starch's thermal stability is unchanged.

Differential scanning calorimetry
The thermal behaviour of the LDPE-starch-(EMA-Zn)-ferric stearate blend is shown in Figure 9. and Table 11., both before to and following biodegradation. The findings show that adding ferric stearate to the blend system has a detrimental impact on the system's crystallinity but only slightly raises the melting temperature. Because there was less of an amorphous phase in the samples, biodegradation may have facilitated the samples' biodegradation and, in turn, helped LDPE crystallize by reducing the amorphous phase. The preferential polymeric chain oxidation that conforms the amorphous phase of the LDPE and the production of new crystallites generated by the chain scission reaction may be responsible for the increase in crystallinity following biodegradation [21].
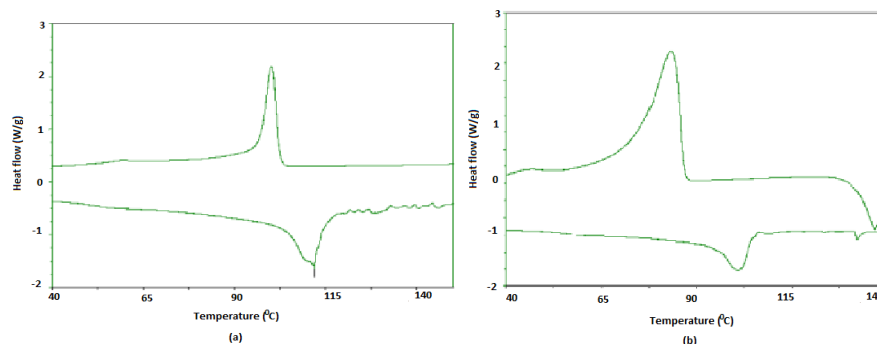
Figure 9. DSC curves of LDPE-starch-(EMA- Zn)-1% ferric stearate blend: (a) before biodegradation and (b) after biodegradation

Table 11.   Results of DSC analysis of LDPE-starch-(EMA-Zn)-1% ferric stearate blend

Sample	T_m (^{0}C)	ΔH_f (J/g)	T_c (^{0}C)	ΔH_c (J/g)	% crystallinity
LDPE	110.00	67.00	96.00	79.00	23.4
LDS-Zn(1)Fe	111.94	59.21	100.16	56.36	20.7
LDS-Zn(1)Fe(ab)	110.99	63.81	93.26	58.92	22.3

Morphological studies
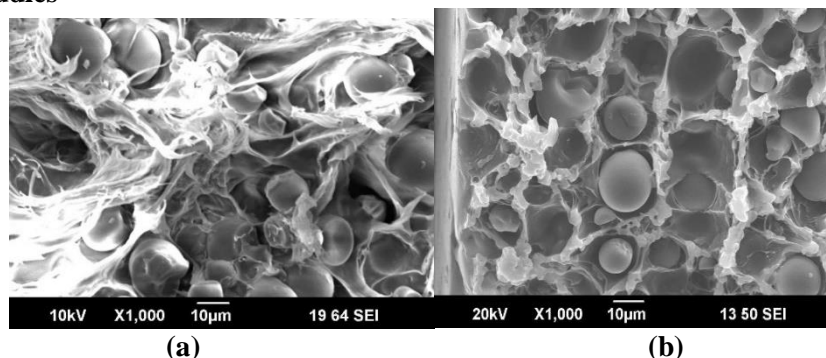

(a)   **(b)**

Figure 10. Scanning electron micrographs of LDPE-starch-(EMA-Zn) blend containing 1% ferric stearate as prooxidant:a) before biodegradation and b) after biodegradation for two months

Figure 10. shows scanning electron micrographs of the cracked surfaces of blends of LDPE-starch-(EMA-Zn)-1% ferric stearate (75/20/5) both before and after they were exposed to biodegradation in culture media. The elimination of starch by microbes causes a number of tiny cavities to become evident in the film after two months of biodegradation [22-23]. However, compared to the LDPE-starch blend, the blend incorporating ferric stearate had fewer holes following biodegradation. This fact suggests that the pro-oxidant ferric stearate has a negative impact on LDPE biodegradation.

CONCLUSIONS
The addition of metal stearates, specifically ferric, manganese, cupric, magnesium, and zinc stearates, to ionomer-compatible LDPE-starch blends improves their tensile strength and elastic modulus while decreasing their elongation at break. On the other hand, the LDPE melt flow index increases when tiny amounts of metal stearates are added. After being immersed in culture medium, the samples' tensile strength significantly decreased, suggesting that microorganisms had biodegraded the mixes. This was further supported by FTIR spectroscopy. As the concentration of metal stearates rises, the ability to absorb water diminishes. When exposed to UV light, blends of LDPE, starch, and ionomer are degraded in the presence of trace amounts of metal stearates. Following photobiodegradation, all of the samples showed a notable decrease in weight and tensile strength. When metal stearates are added, the rate of degradation increases in the following order: FeS > MnS > CuS > MgS. The values of the strorage modulus rose with the addition of metal stearates. The thermal stability and crystallinity of LDPE are altered when trace amounts of metal stearates are added. The pro-oxidant integrated blend samples' biodegradation is verified by SEM micrographs.

Credit authorship contribution statement. Author 1: Methodology, Investigation, Formal Analysis; Author 2: Supervision.

Eur. Chem. Bull. 2022, 11(Regular Issue 1), 608-621

619

Declaration of competing interest. The authors declare that we have no known competing financial interests or personal relationships that could have appeared to influence the work reported in this paper.

REFERENCES

1. Sanniyasi E, Gopal RK, Gunasekar DK, Raj PP. Biodegradation of low-density polyethylene (LDPE) sheet by microalga, Uronema africanum Borge. Scientific reports. 2021;11(1). http://dx.doi.org/10.1038/s41598-021-96315-6. doi:10.1038/s41598-021-96315-6

2. Ammala A, Bateman S, Dean K, Petinakis E, Sangwan P, Wong S, Yuan Q, Yu L, Patrick C, Leong KH. An overview of degradable and biodegradable polyolefins. Progress in polymer science. 2011;36(8):1015–1049. http://dx.doi.org/10.1016/j.progpolymsci.2010.12.002. doi:10.1016/j.progpolymsci.2010.12.002

3. Hamza ZP, Kurian T. Ecoblend: Enhancing compatibility and performance in low-density polyethylene-starch composites with EMA-Zn. Journal of Survey in Fisheries Sciences. 2021. http://dx.doi.org/10.53555/sfs.v8i1.2713. doi:10.53555/sfs.v8i1.2713

4. Ohtake T, Ohtake S, Kobayashi H, Itoh M, Asabe N, Yabuki K, et al. Development of biodegradable LDPE compound and evaluation of its biodegradability. Int Polym Sci Technol. 1995;22(2):49–56.

5. Inceoglu F, Menceloglu YZ. Transparent low-density polyethylene/starch nanocomposite films. J Appl Polym Sci. 2013;129(4):1907–14. DOI: 10.1002/app.38811

6. Oner B, Gokkurt T. Ayse Aytac: Studies on compatibilization of recycled polyethylene/thermoplastic starch blends by using different compatibilizer. Open Chemistry. 2019;17:557–63.

7. Sabetzadeh M, Bagheri R, Masoomi M. Effect of corn starch content in thermoplastic starch/low-density polyethylene blends on their mechanical and flow properties. J Appl Polym Sci. 2012;126(S1). DOI: 10.1002/app.36329

8. Ali A, Xie F, Yu L, Liu H, Meng L, Khalid S, et al. Preparation and characterization of starch-based composite films reinfoced by polysaccharide-based crystals. Compos B Eng. 2018;133:122–8. DOI: 10.1016/j.compositesb.2017.09.017

9. Liang Q, Zhang L, Xiong Y, Wu Q, Tang H. A facile method to prepare a polyethylene glycol modified polysilane as a waterborne photoinitiator. J Photochem Photobiol A Chem. 2015;299:9–17. DOI: 10.1016/j.jphotochem.2014.11.006

10. Roy PK, Surekha P, Rajagopal C, Chatterjee SN, Choudhary V. Accelerated aging of LDPE films containing cobalt complexes as prooxidants. Polymer degradation and stability, 91(8)(2006)1791–1799. http://dx.doi.org/10.1016/j.polymdegradstab.2005.11.010.

11. Jiang T, Duan Q, Zhu J, Liu H, Yu L. Starch-based biodegradable materials: Challenges and opportunities. Adv Ind Eng Polym Res. 2020;3(1):8–18. DOI: 10.1016/j.aiepr.2019.11.003

12. Averous, L.; Fringant, C.; Moro, L. Starch-Based Biodegradable Materials Suitable for Thermoforming Packaging. Starke 2001, 53 (8), 368.

13. Hamza ZP, Anna Dilfi KF, Kurian T, Bhat SG. Biodegradability studies on LDPE-starch blends using amylase-producing vibrios. Int J Polym Mater. 2009;58(5):257–66. DOI: 10.1080/00914030902719386

14. Leewajanakul P, Pattanaolarn R, Ellis JW, Nithitanakul M, Grady BP. Use of zinc-neutralized ethylene/methacrylic acid copolymer ionomers as blend compatibilizers for nylon 6 and low-density polyethylene. J Appl Polym Sci. 2003;89(3):620–9. DOI: 10.1002/app.11898

15. Inceoglu F, Menceloglu YZ. Transparent low-density polyethylene/starch nanocomposite films. J Appl Polym Sci. 2013;129(4):1907–14. DOI: 10.1002/app.38811

16. Rosa, D. S., Grillo, D., Bardi, M. A. G., Calil, M. R., Guedes, C. G. F., Ramires, E. C., & Frollini, E. (2009). Mechanical, thermal and morphological characterization of polypropylene/biodegradable polyester blends with additives. Polymer Testing, 28(8), 836–842. doi:10.1016/j.polymertesting.2009.07.006

17. Lucas, N., Bienaime, C., Belloy, C., Queneudec, M., Silvestre, F., & Nava-Saucedo, J. E. (2008). Polymer biodegradation: Mechanisms and estimation techniques-A review. Chemosphere, 73(4), 429–442.

18. Bremner, T., Rudin, A., & Cook, D. G. (1990). Melt flow index values and molecular weight distributions of commercial thermoplastics. Journal of Applied Polymer Science, 41(7–8), 1617–1627. doi:10.1002/app.1990.070410721

19. Chaoui, S., Smail, D., Hellati, A., & Benachour, D. (2020). Effect of Starch Nanocrystals on the properties of Low Density

Eur. Chem. Bull. 2022, 11(Regular Issue 1), 608-621

620

Polyethylene/Thermoplastic Starch blends. Engineering Technology & Applied Science Research, 10(4), 5875–5881. doi:10.48084/etasr.3608

20. Pedroso, A. G., & Rosa, D. S. (2005). Effects of the compatibilizer PE-g-GMA on the mechanical, thermal and morphological properties of virgin and reprocessed LDPE/corn starch blends. Polymers for Advanced Technologies, 16(4), 310–317. doi:10.1002/pat.581

21. Polińska M, Rozanski A, Galeski A, Bojda J. The modulus of the amorphous phase of semicrystalline polymers. Macromolecules. 2021;54(19):9113–23. DOI: 10.1021/acs.macromol.1c01576

22. Sedláčková M, Lacík I, Chodák I. Poly(ethylene-co-methacrylic acid) copolymer as an effective compatibilizer of LDPE/wood flour composite. Macromol Symp. 2001;170(1):157–64. DOI: 10.1002/1521-3900(200106)170:1<157::aidmasy157>3.0.co;2-n

23. Liu W, Wang Y-J, Sun Z. Effects of polyethylene-grafted maleic anhydride (PE-g-MA) on thermal properties, morphology, and tensile properties of low-density polyethylene (LDPE) and corn starch blends. J Appl Polym Sci. 2003;88(13):2904–11. DOI: 10.1002/app.11965

Eur. Chem. Bull. 2022, 11(Regular Issue 1), 608-621

621